

Two-step effects in 15–35 MeV proton scattering from ^{24}Mg low-lying states

R. De Leo, G. D'Erasmus, E. M. Fiore, and A. Pantaleo
Istituto di Fisica dell'Università di Bari, Bari—Italy,
and Istituto Nazionale di Fisica Nucleare, Sezione di Bari, Italy

M. Pignanelli
Istituto di Fisica dell'Università di Milano, Milano—Italy
and Istituto Nazionale di Fisica Nucleare, Sezione di Milano, Italy

H. V. Geramb
I. Institut für Theoretische Physik, Universität Hamburg, West Germany
 (Received 29 January 1979)

Differential cross sections for proton scattering from the six lowest states of ^{24}Mg have been measured at eleven energies from 15 to 35 MeV. Optical model parameters with a constant geometry and with a linear dependence for the well depths have been deduced for the whole energy range. Coupled channel calculations and the asymmetric rotational model describe satisfactorily the inelastic scattering data of the $K^\pi = 0^+$ rotational band while, in the fits relative to some members of the $K^\pi = 2^+$ band, disagreements have been found. (p,d,p') and (p,p'',p') two-step effects have been considered; the contributions to the $3_2^+(5.22\text{ MeV})$ level data relative to the last process show an energy dependence in agreement with the ^{24}Mg giant resonance strength distributions.

NUCLEAR REACTIONS $^{24}\text{Mg}(p,p')$, $E_p = 15\text{--}35\text{ MeV}$; measured $\sigma(\theta)$ for the six lowest states of ^{24}Mg ; OM, CC, and CN analyses; deduced OM and deformation parameters; microscopic ADWBA including GR resonance effects and (p,d,p') two-step analyses of the $3_2^+(5.22\text{ MeV})$ level data. Enriched target.

I. INTRODUCTION

Whether or not the direct reaction theory is applicable to proton scattering below 20 MeV (Refs. 1 and 2) has been debated for a long time. Recently, however, it has been shown that, even in the incident energy range 20–40 MeV, the proton scattering from low-lying states of low-medium mass nuclei, considered before as a typical direct process, suffers semidirect contributions.^{3–7} Consequently, (p,d,p') or (p,p'',p') two-step processes have been introduced in studying proton scattering. This is on account of the fact that the most important “doorways” in a proton reaction,⁸ and therefore in the first step of the above processes, come from pickup (p,d) and inelastic (p,p') channels.

For medium mass nuclei and for 30 MeV incident energies, calculations including two-step processes with the intermediate particle in a scattering state in the continuum^{8,9} have already been reported. Other models take into account intermediate states in which the incoming particle is captured into a definite resonant state^{4,10} (bound states embedded in the continuum). The fluctuations observed in many (p,p') excitation functions^{3–7} seem to support the thesis^{4,10} that the last

resonant states may be interpreted as giant resonances (GR) of the target.

Scatterings from non-normal parity states are good tools in studying semidirect effects. In fact, the excitation of these states requires a spin-dependent interaction which brings to a strongly hindered direct contribution with better evidence for other reaction mechanisms. In the present work the differential cross sections for proton scattering on ^{24}Mg have been measured at incident energies between 15 and 35 MeV. The transitions leading to excited levels up to 6.01 MeV, and in particular to the unnatural parity state $3_2^+(5.22\text{ MeV})$, have been studied. The experiment is meant to ascertain the presence of semidirect effects at the incident energies able to excite target GR states. It also aims at ascertaining the extent to which the probable semidirect effects may be interpreted as two-step processes which excite, in the intermediate stage, target GR states.

Recent measurements by Youngblood *et al.*¹¹ have positioned the contribution of all isoscalar ^{24}Mg GR, excited in an (α,α') experiment, between 15 and 30 MeV. Similar information is given by (α,γ_0) measurements¹² and by photo-nuclear reactions^{13,14} for the isovector dipolar

GR, hence the validity of the energy range used in this work to investigate GR two-step contributions.

To check the consistency of direct contribution evaluations, a previous measurement¹⁵ at 49.5 MeV on ^{24}Mg has been utilized in this work. At this energy, following hydrodynamic model predictions,¹⁶ GR semidirect effects should vanish. Recently, the proton scattering from ^{24}Mg between 22.5 and 28.5 MeV has been measured by Lovas *et al.*¹⁷ to reach objectives very similar to the ones of this work. But, as can be seen in Refs. 11, 13, and 14, above 22 MeV only a small decaying tail of the GR is excited. In addition, the unfolding of semidirect contributions in Ref. 17 is evaluated in a different way and with a different shell model description of the transition $0_1^- \rightarrow 3_2^-$. However, the last reference constitutes a valid comparison for our study.

In the following, Sec. II briefly describes the experiment. The elastic scattering is analyzed in Sec. III with a standard optical model to deduce a parameter set with a regular energy behavior. Coupled channels and a macroscopic model have been employed in Sec. IV to analyze inelastic scattering data. Compound nucleus contributions affecting data at lower energies have been evaluated in Sec. V. The 3_2^- cross sections have been further interpreted in Sec. VI both with a microscopic antisymmetrized distorted wave calculation and with the predictions of two-step models. Conclusions are summarized in Sec. VII.

II. EXPERIMENTAL PROCEDURE

The measurements were carried out using the analyzed proton beam from the Milan AVF cyclotron. The energy spread of the beam was kept within about 30 keV by means of slits at the exit of the magnetic analyzer. Beams with energy less than 20 MeV, the lowest limit of the accelerator, were obtained by means of beryllium absorbers placed before the analyzer to avoid a beam resolution worsening. No slits were placed at the entrance of the scattering chamber to minimize the background in the spectra especially at small scattering angles. The size of the beam spot in the target region, made visible by an Al_2O_3 foil, was typically 2 mm in diameter.

The target, constituted by an enriched (> 99.98%) self-supporting foil of ^{24}Mg , was $1050 \mu\text{g}/\text{cm}^2$ thick and mounted in the center of a 60 cm scattering chamber. Scattered protons were detected with three counters made up by $5000 \mu\text{m}$ thick silicon totally depleted surface barrier. Thicknesses larger than 5 mm, when needed, were obtained by adding a second, $2000 \mu\text{m}$ thick,

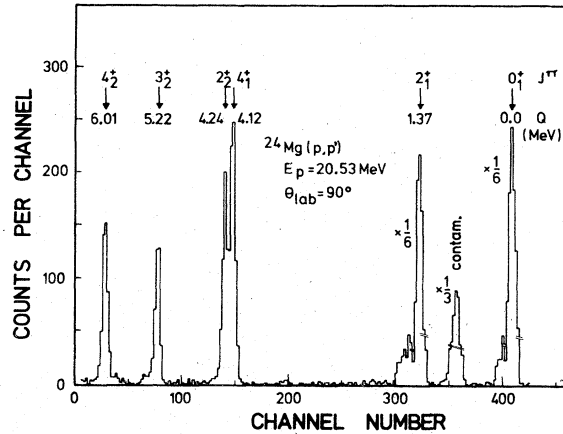


FIG. 1. Typical spectrum of scattered protons.

transmission detector. The solid angle of the counters, defined by a series of tantalum slits, was typically 1 msr defining an angular resolution of near 2° . Angular distributions were measured from 16° to 170° in steps of 6° for the following excited states: g.s. (0_1^+), 1.37 MeV (2_1^+), 4.12 MeV (4_1^+), 4.24 MeV (2_2^-), 5.22 MeV (3_2^-), 6.01 MeV (4_2^-).

A typical proton spectrum, taken at $\theta_{\text{lab}} = 90^\circ$ and $E_p = 20.53$ MeV, is shown in Fig. 1. The overall energy resolution of the data varied from about

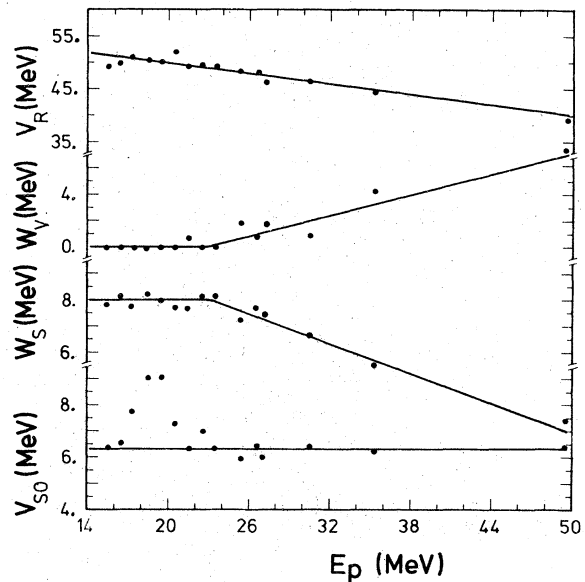


FIG. 2. Well depths obtained in OM analysis and their averaged energy behavior (lines).

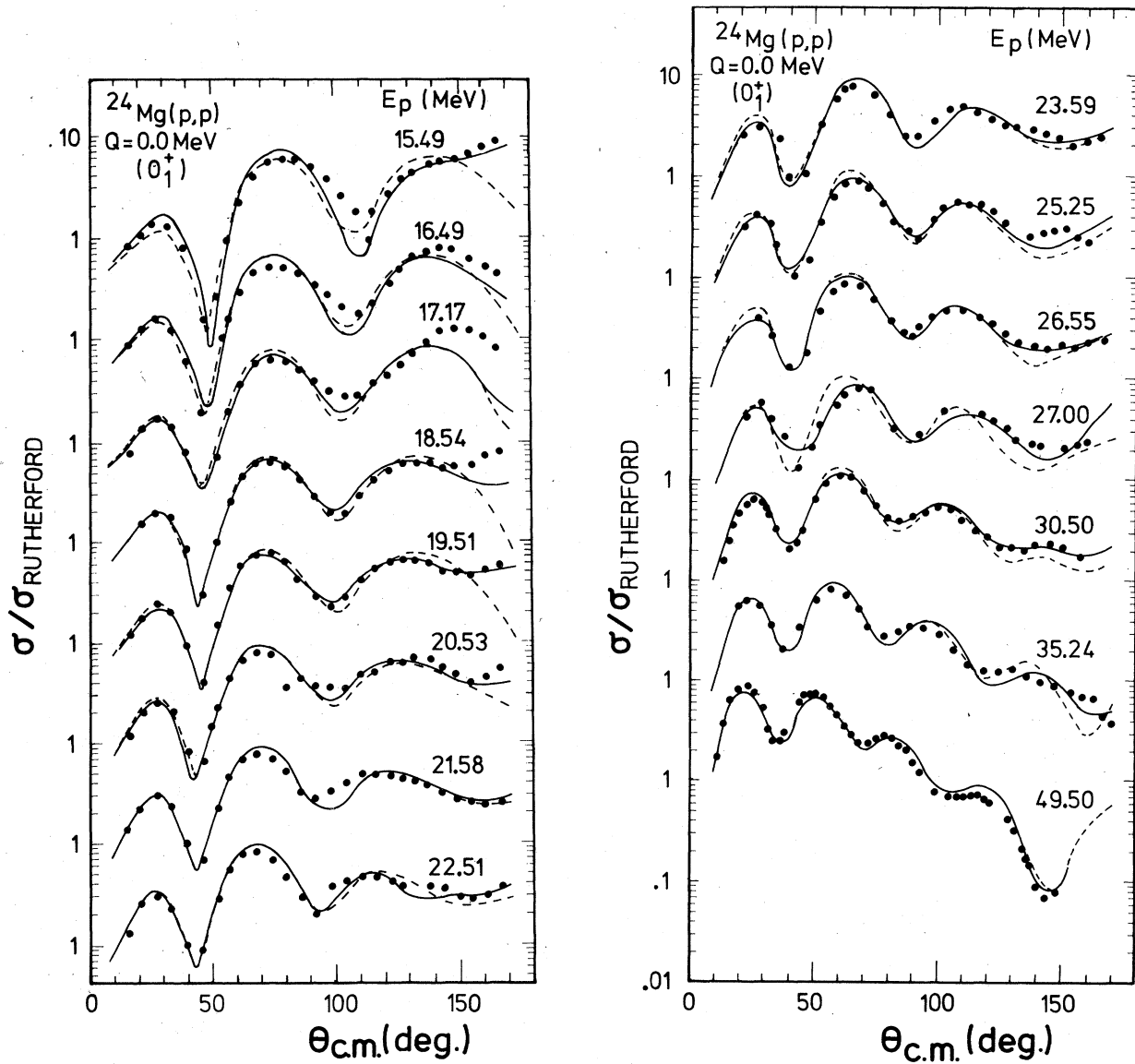


FIG. 3. Proton elastic cross section data together with OM previsions obtained using local (full lines) and energy averaged (dashed lines) potential depths: (a) for incident energies between 15.49 and 22.51 MeV, (b) for incident energies between 23.59 and 49.5 MeV.

100 keV at forward angles of higher energies to about 150 keV at backward angles of lower energies. The target average absorption was considered in determining the effective incident proton energies at which measurements were taken: 15.49, 16.49, 17.17, 18.54, 19.51, 20.53, 21.58, 22.51, 23.59, 26.55, and 35.24 MeV. A small contamination of oxygen in the target was observed and its contribution, hidden at forward angles in the elastic ^{24}Mg peak, was estimated using the data in Refs. 2 and 18. The 4_1^+ and 2_2^+ peaks did not always appear well separated in the spectra; an automatic peak-fitting program was

employed to determine relative intensities. The dead time losses, accounted for in cross section evaluations and, in general, kept below 3%, were accurately determined for each detector.

Statistical errors affecting our data are negligible. Except for the 3_2^+ level data where the background subtraction procedure increased the value to 10%, systematic errors deriving from the overall uncertainties have been estimated at 5%.

III. ELASTIC SCATTERING ANALYSIS

This section aims at deriving optical model (OM) parameters, not influenced by indirect

contributions, in order to evaluate correctly, later on, the direct mechanism contribution in inelastic channels.

At the energies used in this work, many experiments have evidenced resonant effects in proton elastic scattering. A strong anomaly in the energy dependence of the spin-orbit depth has been found for ^{24}Mg , ^{27}Al , ^{28}Si , and ^{32}S by Roy *et al.*⁶ The anomaly appears as a bump superimposed on a constant component positioned at the energy at which the dipolar GR is expected. A similar effect has also been reported by Weller *et al.*¹⁹ on nuclei with very different mass numbers. Finally, in the energy range from 24 to 26 MeV, where the most part of ^{24}Mg GR is already decayed, Lovas *et al.*¹⁷ have found the real and imaginary wells oscillating.

This phenomenology compelled us to avoid searching for different geometrical parameters at each proton energy used and to emphasize a linear energy dependence for well depths. For a better determination of the spin-orbit parameters and of the energy dependence, the polarizations²⁰ at 20.3 and 49.2 MeV and cross sections^{15,17,21} at 25.25, 27, 30, and 49.5 MeV were

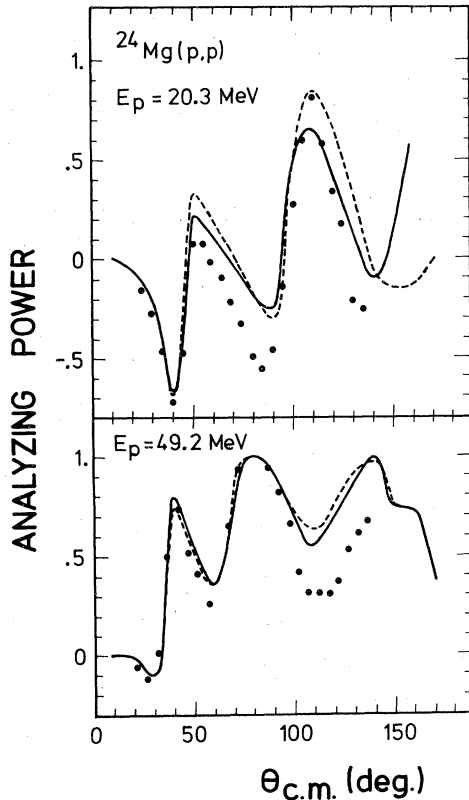


FIG. 4. Proton elastic analyzing powers data together with OM previsions obtained using local (full lines) and energy averaged (dashed lines) potential depths.

included in the analysis. A standard optical potential of the form

$$U(r) = -Vf(x_v) + i4W_D \frac{d}{dx_w} f(x_w) - W_v f(x_w) - \left(\frac{\hbar}{m_\pi c} \right)^2 \frac{1}{2} V_{so} f(x_{so}) + V_c,$$

with $f(x_i)$ Woods-Saxon form factors, and the computer code MERCY by Melkanoff, Raynal, and Sawada, which includes a least-squares routine, were used.

The OM geometry set which caused the overall minimum χ^2 was obtained with multistep grids imposed on each geometrical parameter and with potential depths left free to vary. When polarization data are not included in the analysis, the following geometrical set results: $r_0 = 1.16$, $a_0 = 0.644$, $r_w = 1.3$, $a_w = 0.64$, $r_{so} = 1.1$, $a_{so} = 0.75$ fm. If, however, the fit is also required for polarization data, the previous values change to 1.15, 0.67, 1.35, 0.51, 1.03, 0.6 fm, respectively, causing a worsening of cross section χ^2 of a factor 1.5 on the average. The last geometry caused the values reported in Fig. 2 (points) for the four potential depths and the fits displayed in Figs. 3 and 4 (full lines). In general, the agreement in Fig. 3 is better at forward angles and at higher energies, where nondirect effects are probably less important with respect to the direct contribution. The energy dependences in Fig. 2 are regular for the real and imaginary potentials, while they show the same irregularity found in Ref. 6 for the spin-orbit term. This depth becomes nearly constant from 22 to 50 MeV. Anomalous imaginary depths at 25 MeV, reported in Ref. 17, have not been observed.

Assuming the linear energy behavior for the four depths

$$V_0 \text{ (MeV)} = 56.667 - 0.333 \cdot E_p,$$

$$W_v \text{ (MeV)} = \begin{cases} 0.0 & \text{(for } E_p < 23.0 \text{ MeV)}, \\ 0.27 \cdot E_p - 6.22 & \text{(for } E_p > 23.0 \text{ MeV)}, \end{cases}$$

$$W_s \text{ (MeV)} = \begin{cases} 11.8 - 0.173 E_p & \text{(for } E_p > 23.0 \text{ MeV)}, \\ 7.843 & \text{(for } E_p < 23 \text{ MeV)}, \end{cases}$$

$$V_{so} \text{ (MeV)} = 6.417,$$

shown in Fig. 2 by continuous lines, one obtains an energy dependence very similar to that obtained, for heavier nuclei, by Becchetti and Greenlees.²² The resulting cross sections, drawn in Figs. 3 and 4 with dashed lines, do not show great differences from local determinations (continuous lines) except for the χ^2 values which are a factor 1.5 larger on the average.

We note that the differences between the eval-

uated curves in Fig. 3 concern also the forward angles; therefore, nondirect effects cannot be completely avoided in OM parameter searches excluding the backward part of experimental angular distributions²³ from the fit procedure.

IV. MACROSCOPIC INTERPRETATION OF INELASTIC TRANSITIONS

In this section inelastic data are analyzed with a direct reaction mechanism and a macroscopic model. The aim is to observe the energy dependence of free parameters and to deduce, from their possible anomalous behavior, the presence of nondirect effects.

²⁴Mg, as most nuclei in the 2s-1d shell, is characterized by large static deformations with values²⁴ not yet well defined ($\beta_2 = 0.34, 0.58$; $\beta_4 = -0.05, 0.16$). As collective low-lying states of ²⁴Mg up to 6 MeV excitation are grouped in the rotational bands built on the γ -vibrational state and on the ground state, the application of the rotational model to ²⁴Mg requires the asymmetric version. Obtained values²⁴ for the γ parameter go from 20° to 32°. The first value is also required by Davydov-Filippov calculations²⁵ in reproducing the ²⁴Mg level sequence.

On account of the large ground-state deformation of ²⁴Mg the analysis of inelastic scattering data cannot be performed unless the higher order processes deriving from the strong coupling among the rotational states are kept in consideration. A coupled channels (CC) method is required; to this end the Raynal computer program ECIS has been used. The code includes a routine to search for OM parameters and deformations. Moreover, when it is used in the asymmetric rotational version, following the Davydov-Filippov model,²⁵ it allows a mixing between the two bands $K^\pi = 0^+$ and 2^+ with coefficients evaluated by the code itself from the γ value.

Several runs of the program have ascertained the following:

(i) A variation of γ causes negligible effects both on cross section shapes and absolute values; the value $\gamma = 21^\circ$ was used in subsequent analyses.

(ii) It is necessary to reduce by a relevant quantity the imaginary potential deduced from OM analyses since, in this CC calculation, the imaginary term no longer accounts for many inelastic transitions. Only the surface part of the potential was varied and fixed to the final values: $W_s = 5.2$ MeV (for $E_p < 23$ MeV); $W_s = (8.42 - 0.14 E_p)$ MeV (for $E_p > 23$ MeV).

(iii) The hexadecapole deformation inclusion brings no significant improvement to the fits,

and, in particular, to the 4^+ states notwithstanding the levels can be directly excited from the ground state.

(iv) β_4 comes out strongly correlated to β_2 . When a search is imposed on β_4 only, with β_2 fixed at 0.5, the values reported in the upper part of Fig. 5 result for β_4 ; however, little confidence should be attributed to them since they strongly depend upon the assumption made for other parameters.

A search on β_2 , performed with equal weights attached to all cross sections and including available analyzing powers,²⁰ brought us to the values shown in the lower part of Fig. 5 (points). β_2 is constant and equal to 0.48 from 21 and 50 MeV and fluctuates at lower energies. When the compound nucleus contribution, as estimated in the following section, is subtracted from the experimental points, also at the lowest energies, β_2 becomes constant and equal to its high energy value with the exception of the 19.5 and 20.5 MeV determinations (square dots in Fig. 5).

Evidence of a dominant direct effect is obtained in the regular behavior of β_2 for most of the energies studied. When the data at 18.54, 19.51, and 20.53 MeV are excluded, since fluctuations are present in them, the average values for the deformation parameters which result are $\beta_2 = 0.486 \pm 0.008$ and $\beta_4 = 0.05 \pm 0.04$. The quoted errors give the standard deviations of results in Fig. 5. The CC fits obtained, shown at three incident energies in Fig. 6, are good at each angle and energy for the $K^\pi = 0^+$ band and for the 2_2^+ state. A different situation exists for the transitions to the other levels of the $K^\pi = 2^+$ band, for which the shape of the angular distribution is not reproduced. To account for their absolute values, the curves calculated must be renormalized by large factors. In agreement with Refs. 17 and 26,

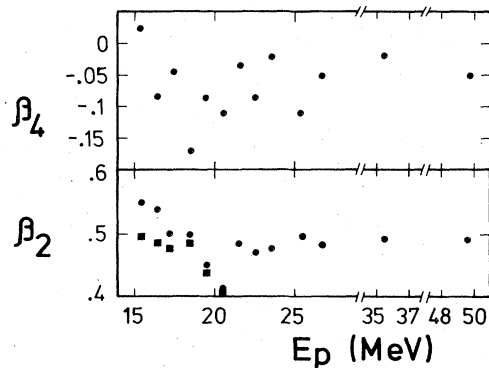


FIG. 5. Hexadecapole and quadrupole deformation values extracted from CC analyses described in the text, with (points) and without (squares) CN contributions.

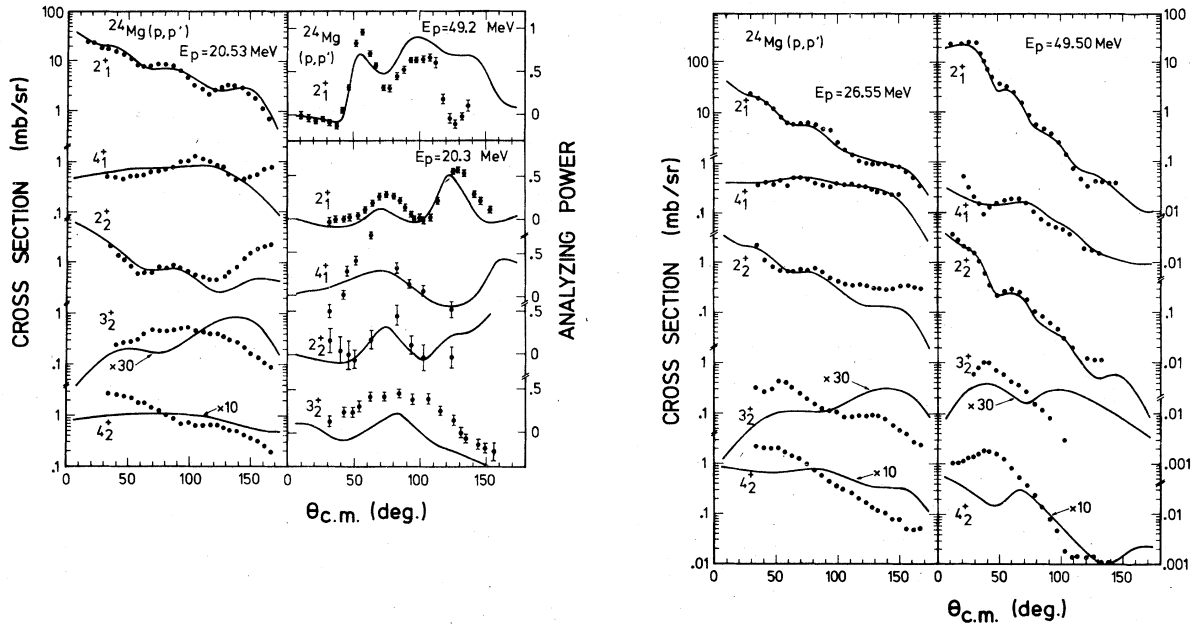


FIG. 6. (a) CC fits to cross sections at 20.53 MeV and to analyzing powers at 20.3 and 49.2 MeV. (b) CC fits to cross sections at 26.55 and 49.5 MeV.

the factors required are about 25–30 and 6 for the transitions to the 3_2^+ and to the 4_2^+ state, respectively. Moreover, when compound nucleus contributions, evaluated as described in the next section, are subtracted from the experimental data, the normalization factors result slightly decreasing with the energy.

Thus the presence of other reaction mechanisms seems plausible, at least for the 4_2^+ and 3_2^+ transitions. It would be interesting to attempt a different description of the direct process for the latter transition since its disagreement with CC predictions is very large.

V. COMPOUND NUCLEUS CONTRIBUTIONS

To evidence the starting point of two-step processes, measurements in this work have been taken from 15.5 MeV. At such low incident energies compound nucleus (CN) contributions may be present in the data and then they must be singled out in the cross section to avoid their interpretation in terms of two-step effects in subsequent analyses.

We have estimated CN contributions using the Hauser-Feshbach (HF) expression reported in Ref. 27. The transmission coefficients for proton, neutron, deuteron, and α CN decay channels have been described by the OM parameters reported in Table I and taken from Refs. 28, 29, and 30. The level densities for residual nuclei have been calculated using the Fermi-gas model formula³¹ with the back shift for their energy scale reported in Ref. 32, and taking the pairing energies from Ref. 33.

On account of the uncertainties in the above parameters for a light nucleus, little reliability should be attached to absolute values of the CN calculations. To test the latter, we have compared HF previsions summed to CC direct contributions, with the experiment. Since in several cases the evaluated sum exceeds the data, the CN contributions seem overevaluated. Comparison with the data is more significant for the transitions leading to 2^+ and 4_1^+ levels, for which the evaluation of the direct effect by a CC seems to be more reliable. In particular, the results of measurements at 15 MeV, taken with an energy resolution

TABLE I. Optical model parameters used to evaluate CN contributions.

Channel	V	r_v	a_v	W_D	r_w	a_w	V_{so}	r_{so}	a_{so}	r_c	Ref.
proton	$55.67 - 0.33E_p$	1.15	0.67	7.84	1.35	0.51	6.4	1.15	0.67	1.2	Present work
alpha	147.0	1.7	0.55	6.25	1.7	0.55	1.4	28
neutron	$47.0 - 0.267E_p - 0.0018E_p^2$	1.31	0.66	$9.52 - 0.05E_p$	1.26	0.48	7.0	1.31	0.66	...	29
deuteron	100.41	1.05	0.86	26.95	1.43	0.61	5.2	1.05	0.86	1.3	30

of 400 keV to average the Ericson statistical fluctuations evidenced in neighboring nuclei,³⁴ require a CN contribution reduced by a factor of 0.4 (see Fig. 7). More evidence for this reduction comes from the 9 MeV data³⁵ which are exceeded by CN evaluations only (Fig. 7), and from similar results found in the same last reference also for ^{25,26}Mg.

Following Hodgson and Wilmore,³⁶ a normalization factor lower than 1 may also account for the loss of particles involved in the direct mode before the compound stage is reached. No attempts to better determine HF predictions by comparing them to transfer reaction cross sections have been made for the lack of measurements at the required energies.

CN contributions thus evaluated are comparable with the experimental yields only for the 3_2^+ and 4_2^+ transitions at the lowest energies. However, above 18 MeV, the CN contributions are no longer an important component also for the two foregoing transitions. This is on account of their decrement with the energy (a factor of 10 every 5 MeV), faster than the experimental data one. The limit is increased to 22 MeV when the 0.4 normalization factor is neglected.

VI. 3_2^+ DATA ANALYSES

The notable disagreement found between macroscopic calculations and 3_2^+ data could indicate that the high order processes involving couplings with low-lying collective states are not suitable for describing the reaction mechanism of this transition.

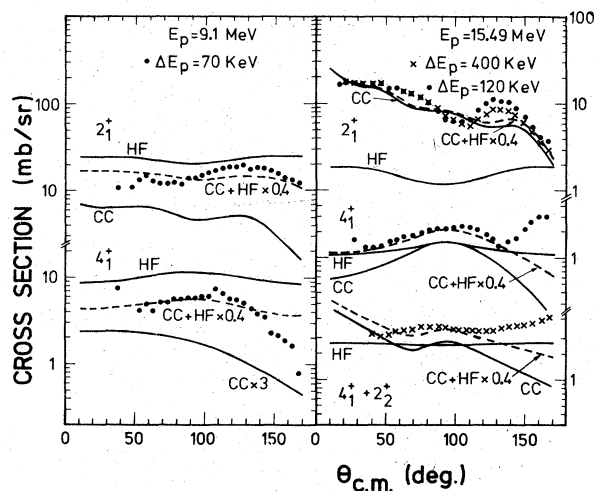


FIG. 7. Differential cross sections for the reaction $^{24}\text{Mg}(p, p')$ on various excited levels measured with a high (points) and low (crosses) resolution energy. Curves represent compound nucleus (HF), direct reaction (CC) contributions, and their sum.

The 3_2^+ state can be directly excited from the ground state by a spin-flip mechanism ($\Delta S = 1$). To evaluate this, a microscopic antisymmetrized distorted wave (ADWBA) calculation has been performed by means of the MEPHISTO code.¹⁰ Valence and core polarization effects are included in its transition amplitude made up of a coherent sum of single particle amplitudes. Each of them is weighed through a spectroscopic factor specified by the nuclear structure of the levels involved. Similar calculations have been described in detail elsewhere.^{4,10}

For the present analysis the spectroscopic amplitudes have been taken from a recent evaluation (Table II) obtained by Wildenthal diagonalizing a Hamiltonian in the full $2s-1d$ shell space. The valence interaction operator is given by a linear mixture of central, tensor, and spin-orbit components, each with a Gaussian type finite range form factor. The central part of this interaction is equivalent to the long range part of the Hamada-Johnston potential.³⁷ The non-central components are based on the Eikemeier and Hackenbroich force.³⁸ The distorted waves for the incoming and outgoing channels were generated from an optical model calculation with parameters taken from Sec. III. The bound orbitals were taken as oscillator states with the strength fixed at 10.6 MeV.

The evaluated valence contributions, including the antisymmetrization term, are reported in Fig. 8 with dashed lines at only three sample energies. The order of magnitude of cross section values is now reproduced at the higher energies. This denotes a relatively strong contribution coming from the direct spin-flip excitation. However, the shape of the angular distribution is poorly reproduced. This fact may be due either to an unsatisfactory spectroscopic description or to the presence of other processes besides the direct one. At energies less than 30 MeV the valence contribution no longer reproduces the

TABLE II. Spectroscopic amplitudes for the $0_1^+ - 3_2^+$ transition in ^{24}Mg .

$n_1, l_1, j_1 - n_2, l_2, j_2$	S
$d_{5/2} \quad d_{5/2}$	-0.1645
$d_{5/2} \quad 2s_{1/2}$	0.3540
$d_{5/2} \quad d_{3/2}$	-0.1219
$2s_{1/2} \quad d_{5/2}$	-0.1632
$2s_{1/2} \quad 2s_{1/2}$...
$2s_{1/2} \quad d_{3/2}$...
$d_{3/2} \quad d_{5/2}$	-0.0845
$d_{3/2} \quad 2s_{1/2}$...
$d_{3/2} \quad d_{3/2}$	-0.1305

absolute values of the cross sections observed; at 17.17 MeV a normalization of the order of 10 must be introduced. The energy dependence of the necessary renormalization factors is reported in Fig. 9. To better explain the experiment, other reaction mechanisms should be taken into account, in particular those with a yield larger in the energy region below 26 MeV.

As shown in Ref. 8 inelastic two-step processes (p, p'', p') with the intermediate proton in the continuum provide the maximum yield when the intermediate p'' proton is at about 10 MeV of kinetic energy. Considering that high-lying collective states, reached by the target in the intermediate step, are clustered at GR energies, i.e., at about 20 MeV for ^{24}Mg , one can predict that the above process gives the maximum contribution at about 30 MeV. Therefore it will not be

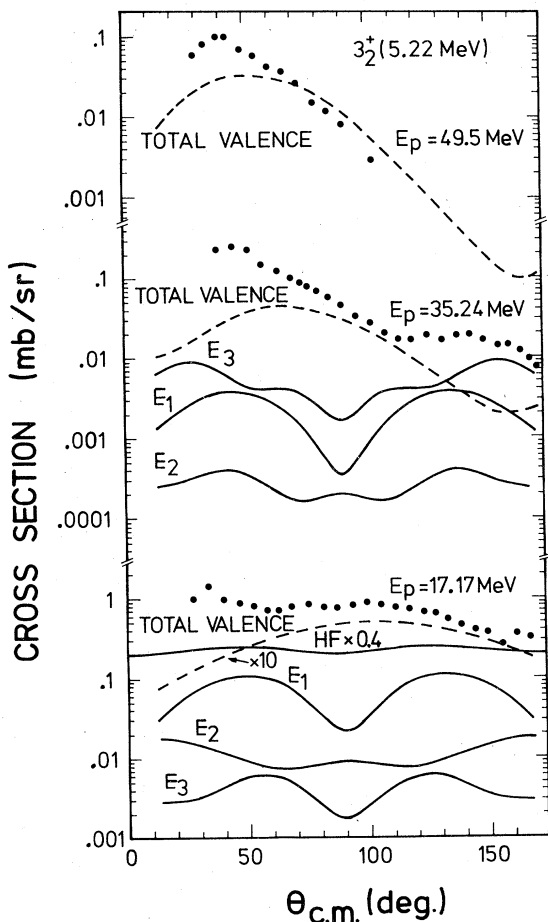


FIG. 8. Total valence contributions to the 3_2^+ cross sections at 49.5, 35.24, and 17.17 MeV. Core exchange curves (E_1 , E_2 , E_3), arbitrarily normalized, are also given. The CN contribution (HF), as evaluated in Sec. V, is given for the cross section at 17.17 MeV.

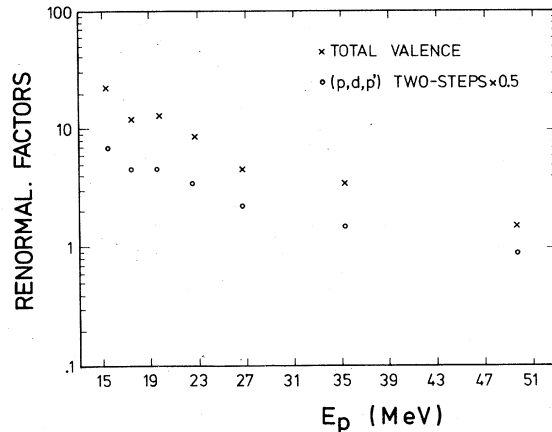


FIG. 9. Total valence and (p, d, p') two-step renormalization factors necessary to reproduce the 3_2^+ experimental yield.

considered in the following.

Following Mackintosh,⁹ the (p, d, p') process should display a maximum in the excitation function, positioned at about 11 MeV for the intermediate deuteron. The same should be the dominant two-step process among the ones with an intermediate particle in the continuum.^{8,9} Taking into account the threshold energy for the (p, d) reaction, the maximum yield for the (p, d, p') process should be obtained in the energy interval of 26–31 MeV, and is therefore of no use for our 3_2^+ study. However, the energy dependence of the (p, d, p') process calculated by us has resulted in one similar to the direct effect one (see Fig. 9). The calculation has been carried out by using the Kunz code CHUCK and spectroscopic amplitudes consistent with the (p, d) study of Kozub.³⁹ The points given in Fig. 9 for the (p, d, p') effect have been calculated with the OM parameters for deuteron channels given in Ref. 40, and similar results have been obtained by using the OM prescriptions of Johnson and Soper.⁴¹ The (p, d, p') cross section absolute value results are similar to or slightly larger than the direct spin-flip contribution. However, owing to effects of nonorthogonality,⁴² the (p, d, p') calculation may be overestimated.

Therefore, the inclusion of the pickup-stripping process could give some sizable contribution to the calculated cross sections, but, when added to CN and direct effects, it is not able to restore the 3_2^+ experimental energy dependence.

A process which has instead a maximum yield at 18–26 MeV should be a two-step process via intermediate resonant states if the latter are identified in the dipolar and quadrupolar GR. This process is included in the MEPHISTO code and is formally described by the exchange core

polarization term. The direct part of the core polarization term accounts for the omitted valence contribution due to the necessity of using a simplified and incomplete spectroscopy for target states. However, for a spin-flip transition this term is not allowed.⁴³ The exchange term is evaluated by using a collective model representation.¹⁰ It considers processes in which the incident particle is trapped into a spectator bound state with the required energy, momentum, and isospin transfer, exciting resonancelike states in the target which subsequently decay by a particle emission into the continuum:

$$T_{sp} = \sum_{\lambda\mu} y_{\lambda}(\bar{Q}) \langle \chi^{-}(0) | V_{\lambda\mu}(0) | \phi_{j_1}(0) \rangle \\ \times \langle \phi_{j_1}(1) | V_{\lambda\mu}(1) | \chi^{+}(1) \rangle,$$

where

$$y_{\lambda}(\bar{Q}) = Y_{\lambda}(\bar{Q}) e^{i\phi_{\lambda}(\bar{Q})} \\ = - \frac{\beta_{\lambda}^2}{2\lambda + 1} (\bar{Q} - \hbar\omega_{\lambda} + \frac{1}{2}i\Gamma_{\lambda})^{-1}.$$

The intermediate states in this process have centroid energies $\hbar\omega_{\lambda}$ and resonance widths

Γ_{λ} . \bar{Q} is the sum of the incident energy and the spectator binding energy. β_{λ} is the usual collective model deformation parameter which measures the total transition strength to form the intermediate λ multipolarity level from the ground state. When these states are interpreted as target collective GR, the values allowed for β_{λ} may be constrained by the energy weighted sum rules⁴⁴ (EWSR). The strengths $Y_{\lambda}(\bar{Q})$ and phases $\phi_{\lambda}(\bar{Q})$ of these contributions have been treated as adjustable parameters in a search process to fit the experimental cross sections. In principle all multipoles can contribute, but generally a small number of terms is retained in the search procedure.

In the search performed in this work the dipolar, quadrupolar, and octupolar multipoles have been introduced. The last contribution was not included in previous works,^{4,17} but the proof of the presence of E3 GR in the interval explored is drawn from the following works: (i) Yang *et al.*⁴⁵ found 10% of the octupole EWSR strength in the excited states of ²⁴Mg up to 16 MeV; (ii) Van der Borg *et al.*⁴⁶ found several states with angular distributions reproduced by an $L=3$

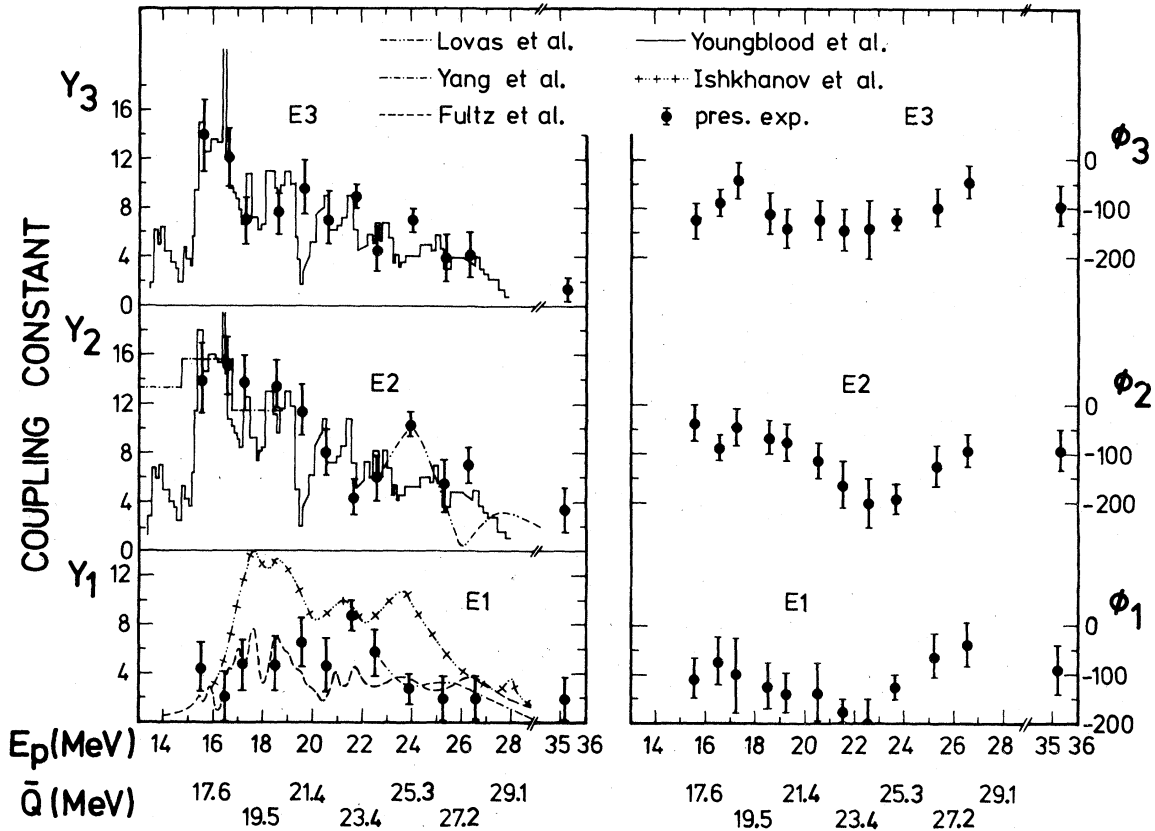


FIG. 10. Variation with the incident (E_p) and excitation (\bar{Q}) energies of the core exchange E1, E2, E3 coupling constants (points) determined from the fits in Fig. 11. The curves represent the GR strength distribution in ²⁴Mg.

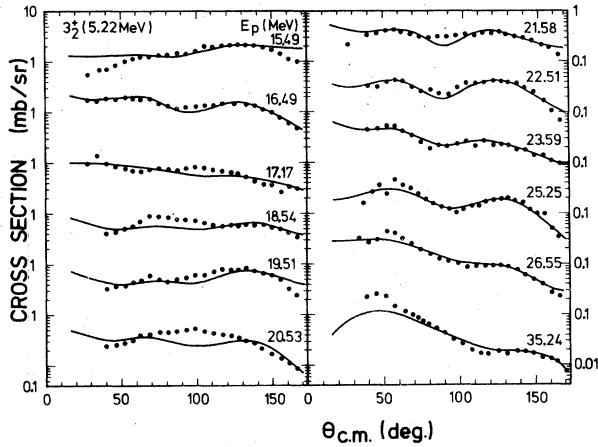


FIG. 11. Differential cross sections for the inelastic proton scattering from the 3_2^+ state of ^{24}Mg ; curves represent the result of a microscopic ADWBA calculation in which two-step GR processes have been included.

calculation in a high resolution α -scattering study of the ^{28}Si GR region.

The shapes of the $L=1, 2, 3$ core exchange contributions to the 3_2^+ cross sections are shown, arbitrarily normalized, in Fig. 8. They appear sufficiently different among themselves to ensure an unambiguous choice of the multiplicities excited in the intermediate stage. Their contributions (modules and phases) necessary in reproducing the experimental data are shown in Fig. 10, while the fits obtained are displayed in Fig. 11. The curves drawn in Fig. 10 represent ^{24}Mg $E1$ and $E2$ GR strength distributions as taken from Refs. 11, 13, 14, and 17; they are in sufficient agreement with our deduction.

Little confidence may be had in the absolute values obtained for the different multipole strengths. This is a consequence of the uncertainties concerning the direct and two-step evaluation, and of the omission of other reaction mechanisms such as the (p, d, p') one. These uncertainties are, however, smaller in the energy region between 15 and 23 MeV, where ^{24}Mg GR states are positioned and where the direct and (p, d, p') processes have been found to be responsible for some 10% of the total effect.

The method suggested by Perrin *et al.*⁴⁷ has been used to roughly estimate the EWSR fractions⁴⁸ present in the strengths of Fig. 11. They are 30%, 100%, and 20% of the $E1$, $E2$, and $E3$ EWSR, respectively, supposing the two last GR

to be only isoscalar in character. Considering that below 16 MeV Yang *et al.*⁴⁵ found another 30% of the isoscalar $E2$ strength, the $E2$ percentage here found appears large. This fact may be due to the above cited omission of other reaction mechanisms, but also, as suggested by Lovas *et al.*,¹⁷ to the presence of an isovector component of ^{24}Mg $E2$ GR.

VII. CONCLUSION

We have reported here the differential cross sections for the proton scattering from the ^{24}Mg six lowest states at incident energies between 15 and 35 MeV, an interval that involves different reaction mechanisms.

A CC calculation and the asymmetric rotational model have been used to describe the transitions leading to the $K^\pi=0^+$ band states. The angular distributions, both for cross sections and for polarizations, and the cross section energy dependences are reasonably well described. The average values deduced for the collective parameters are $\gamma=21^\circ$, $\beta_2=0.486\pm 0.008$, and $\beta_4=0.05\pm 0.04$. However, the same CC calculation has not described the data of the $K^\pi=2^+$ rotational band. The disagreement is particularly evident for the transition to the 3_2^+ state. This level, slightly excited by the direct mode, which is usual for an unnatural parity state, emphasizes other reaction mechanisms.

Possible mechanisms, coming from couplings with the low- or high-lying collective states or with deuteron channels, cannot be excluded. We have estimated that these mechanisms give sizable contributions at each incident energy in comparison to the evaluated direct process, and, at least above 30 MeV, also in comparison to the experimental cross section. However, the description of the 3_2^+ energy dependences is not improved by the introduction of these latter processes. To this end the two-step process via a GR state, supplementing the direct spin-flip mode, seems more suitable. The reliability of this hypothesis has been proved *a posteriori* by a comparison of the energy distribution of dipole and quadrupole GR strengths, as needed to fit the 3_2^+ data and as deduced from photonuclear and α scattering experiments.

We thank Mr. P. Tempesta and Dr. M. Tarantino for technical support.

- ¹C. B. Duke, Phys. Rev. **129**, 681 (1963).
- ²W. W. Daehnick, Phys. Rev. **135**, B1168 (1964).
- ³C. R. Lamontage, B. Frois, R. J. Slobodrian, H. E. Conzett, C. Leemann, and R. DeSwinarski, Phys. Lett. **45B**, 465 (1973); H. R. Weller and M. Divadeenam, *ibid.* **55B**, 41 (1974).
- ⁴H. V. Geramb, K. Amos, R. Sprickmann, K. T. Knöpfle, M. Rogge, D. Ingham, and C. Mayer-Böriche, Phys. Rev. C **12**, 1697 (1975).
- ⁵R. DeLeo, G. D'Erasmus, F. Ferrero, A. Pantaleo, and M. Pignanelli, Nucl. Phys. **A254**, 156 (1975).
- ⁶R. Roy, C. R. Lamontagne, R. J. Slobodrian, J. Arvieux, J. Birchall, R. M. Larimer, and H. C. Conzett, in *Proceedings of the International Conference on Nuclear Structure, Tokyo, 1977* (International Academic, Tokyo, Japan, 1977), p. 492.
- ⁷R. DeLeo, G. D'Erasmus, A. Pantaleo, G. Pasquariello, G. Viesti, M. Pignanelli, and H. V. Geramb, Phys. Rev. C **19**, 646 (1979).
- ⁸P. W. Coulter and G. R. Satchler, Nucl. Phys. **A293**, 269 (1977); C. L. Rao and G. R. Satchler, *ibid.* **A207**, 182 (1973).
- ⁹R. S. Mackintosh, Nucl. Phys. **A209**, 91 (1973); R. S. Mackintosh and A. M. Kobos, Phys. Lett. **62B**, 127 (1976); R. S. Mackintosh and A. M. Kobos, report, 1978 (unpublished).
- ¹⁰H. V. Geramb, R. Sprickmann, and G. L. Strobel, Nucl. Phys. **A199**, 545 (1973).
- ¹¹D. H. Youngblood, C. M. Rozsa, J. M. Moss, D. R. Brown, and J. D. Bronson, Phys. Rev. C **15**, 1644 (1977).
- ¹²E. Kuhlmann, E. Ventura, J. R. Colarco, D. G. Mavis, and S. S. Hanna, Phys. Rev. C **11**, 1525 (1975).
- ¹³S. C. Fultz, R. A. Alvarez, B. L. Berman, M. A. Kelly, D. R. Lasher, T. W. Phillips, and J. McElhinney, Phys. Rev. C **4**, 149 (1971).
- ¹⁴B. S. Ishkhanov, I. M. Kapitanov, V. G. Shevchenko, and B. A. Yurev, Izv. Akad. Nauk. SSSR, Ser. Fiz. **30**, 378 (1966) [Bull. Acad. Sci. USSR, Phys. Ser. **30**, 383 (1966)].
- ¹⁵A. A. Rush, E. J. Burge, V. E. Lewis, D. A. Smith, and N. K. Ganguly, Nucl. Phys. **A104**, 340 (1967).
- ¹⁶A. Bohr and B. R. Mottelson, *Nuclear Structure* (Benjamin, New York, 1975), Vol. II.
- ¹⁷I. Lovas, M. Rogge, U. Schwinn, P. Turek, and I. Ingham, Nucl. Phys. **A286**, 12 (1977).
- ¹⁸D. Karban, P. D. Greaves, V. Hnizdo, J. Lowé, N. Berovic, H. Wojciechowski, and G. W. Greenlees, Nucl. Phys. **A132**, 548 (1969).
- ¹⁹H. R. Weller, J. Szües, J. A. Kuehner, G. D. Jones, and D. T. Petty, Phys. Rev. C **13**, 1055 (1976).
- ²⁰V. E. Lewis, E. J. Burge, A. A. Rush, D. A. Smith, and N. K. Ganguly, Nucl. Phys. **A101**, 589 (1967); A. G. Blair, G. Glahausser, R. DeSwinarski, J. Goudergues, R. Lombard, B. Mayer, J. Thirion, and P. Vaganov, Phys. Rev. C **1**, 444 (1970).
- ²¹J. Eenmaa, R. K. Cole, C. N. Waddell, H. S. Saudhu and R. R. Dittman, Nucl. Phys. **A218**, 125 (1974); I. Lovas, M. Rogge, U. Schwinn, P. Turek, D. Ingham, and C. Mayer-Böriche, Jülich report, 1974 (unpublished), p. 13.
- ²²F. D. Becchetti and J. W. Greenlees, Phys. Rev. **182**, 1190 (1969); C. M. Perey and F. G. Perey, At. Data Nucl. Data Tables **17**, 1 (1976).
- ²³R. Sprickmann, K. T. Knöpfle, D. Ingham, M. Rogge, C. Mayer-Böriche, and H. V. Geramb, Z. Phys. **A274**, 339 (1975).
- ²⁴A. Kiss, O. Aspelund, G. Hrehuss, K. T. Knöpfle, M. Rogge, U. Schwinn, Z. Seres, P. Turek, and C. Mayer-Böriche, Nucl. Phys. **A262**, 1 (1976).
- ²⁵W. F. Hornyak, *Nuclear Structure* (Academic, New York, 1975), p. 399.
- ²⁶R. M. Lombard, J. L. Escudie, and M. Soyeur, Phys. Rev. C **18**, 42 (1978).
- ²⁷H. Feshback, in *Nuclear Spectroscopy*, edited by F. Ajzenberg-Selove (Academic, New York, 1960), p. 625.
- ²⁸J. R. Huizenga and G. Igo, Nucl. Phys. **29**, 462 (1962).
- ²⁹D. Wilmore and P. E. Hodgson, Nucl. Phys. **55**, 673 (1964).
- ³⁰J. M. Lohr and W. Haerberli, Nucl. Phys. **A232**, 381 (1974).
- ³¹J. M. B. Lang and K. J. Le Couteur, Proc. Phys. Soc. London **A67**, 585 (1965).
- ³²E. Gadioli and L. Zetta, Phys. Rev. **167**, 1016 (1968).
- ³³A. G. W. Cameron, Can. J. Phys. **36**, 1040 (1958).
- ³⁴K. W. Kemper, J. D. Fox, and D. W. Oliver, Phys. Rev. C **5**, 1527 (1972); G. D. Gum, K. W. Kemper, and J. D. Fox, Nucl. Phys. **A232**, 176 (1974).
- ³⁵M. Herman, A. Marciukowski, B. Zwieglinski, W. Augustyniak, J. Bielewicz, and W. Zych, J. Phys. **G2**, 831 (1976).
- ³⁶P. E. Hodgson and D. Wilmore, Proc. Phys. Soc. London **90**, 361 (1967).
- ³⁷T. Hamada and D. Johnston, Nucl. Phys. **34**, 382 (1962).
- ³⁸H. Eikemeier and H. H. Hackenbroich, Nucl. Phys. **A169**, 407 (1971).
- ³⁹R. L. Kozub, Phys. Rev. **172**, 1078 (1968).
- ⁴⁰F. Hinterberger, G. Mairle, V. Schmidt-Rohr, G. J. Wagner, and P. Turek, Nucl. Phys. **A111**, 256 (1968).
- ⁴¹R. C. Johnson and P. J. Soper, Phys. Rev. C **1**, 976 (1970).
- ⁴²D. Robson, Phys. Rev. C **7**, 1 (1973); P. P. Kunz and E. Rost, Phys. Lett. **47B**, 136 (1973); T. Udagawa, H. H. Volter, and W. R. Coker, Phys. Rev. Lett. **31**, 1507 (1973).
- ⁴³W. G. Love and G. R. Satchler, Nucl. Phys. **A101**, 424 (1967); **A172**, 449 (1971).
- ⁴⁴G. R. Satchler, Phys. Rep. **14C**, 98 (1974).
- ⁴⁵G. C. Yang, P. P. Singh, A. Van Der Wonde, and A. G. Drentje, Phys. Rev. C **13**, 1376 (1976).
- ⁴⁶K. Van Der Borg, M. N. Harakch, S. Y. Van Der Werf, A. Van Der Wonde, and F. E. Bertrand, Phys. Lett. **67B**, 405 (1977).
- ⁴⁷G. Perrin, D. Lebrun, J. Chauvin, P. De Santignon, D. Eppel, H. V. Geramb, H. L. Yadov, and V. A. Madsen, Phys. Lett. **68B**, 55 (1977).
- ⁴⁸A. M. Bernstein, in *Advances in Nuclear Physics*, edited by M. Baranger and E. Vogt (Plenum, New York, 1969), Vol. III, p. 325.